TechnoChem
International Journal of TechnoChem Research
ISSN:2395-4248 www.technochemsai.com
Vol.02, No.03, pp 224-238, 2016

Photocatalytic Applications of AG DOPED-ZNO Nano Particles Driven by Light Emitting Diodes (Led) Illumination.

Y Jerlin Jose[1,3], M Manjunathan[1,2] and S Joseph selvaraj[3]

[1]Department of chemistry, BWDA Arts and science college, Tindivanam-604304 India
[2]Department of chemistry, Pondicherry University Pondicherry 605014 India
[3]Department of chemistry, St. Josephs college, Tiruchirappalli-620002 India

Abstract : A simple precipitation-decomposition method to synthesized Ag–ZnO nano particles successfully. The synthesized photocatalyst was characterized by XRD, SEM,INFRARED SPECTROSCOPY and ULTRAVIOLET-VISIBLE spectroscopy.
The photocatalytic activity of Ag–ZnO was investigated by photodegradation of methylene blue. Ag–ZnO photocatalyst is found to be more efficient than bare ZnO, commercial ZnO, and TiO_2 nano powers. Silver dopants shift the absorbance of ZnO to the visible region (353-361 nm). The influences of operational parameters such as initial pH, amount of photocatalyst and dye concentration on photo-mineralization of MB have been analyzed. A degradation mechanism is proposed for the degradation of MB under LEDs.

1. Introduction

Contamination of water and to control that contamination is indispensable need to prevent this universe. These Contamination is due to organic matter poses severe threat to life on the earth [1]. Dyes occupies primary part in contaminating and polluting the waters. Dyes are coloured substance which have many chemical compounds which is poisonous in nature. The unwanted chemicals should be removed from the dye in order to purify the water. The polluted water gives adverse-effect[2].

The use of semiconductors has attracted for the photodegradation of organic pollutants[3-6].

The general scheme for the photocatalytic destruction of organic compounds involves the following three steps: (i) when the energy hυ of a photon is equal to or higher than the band gap (Eg) of the semiconductor, an electron is excited to conduction band, with simultaneous generation of a hole in the valance band; ii) then the photoexcited electrons and holes can be trapped by the oxygen and surface hydroxyl, respectively, and ultimately produce the hydroxyl radicals (•OH), which are known as the primary oxidizing species; and (iii) the hydroxyl radicals commonly mineralize the adsorbed organic substances.

TiO_2 is the best photocatalyst for the degradation process[7-9].The photocatalytic degradation is done in the presence of natural sunlight or mercury vapor lamp and LED [10-14]. Photo catalyst can remove all the toxic chemicals. TiO_2 and ZnO are good semiconductors used as photocatalyst. ZnO nanocatalyst is also can be used as an alternative for TiO_2 [15-17].

ZnO is a dilute magnetic semiconductor. ZnO is having a good chemical and thermal stability. ZnO based DMS have the band gap energy 3.37ev at room temperature, large excitation binding energy of 60Mev[18,19]. So ZnO is a very good alternative for other semiconductors. ZnO can produce point defects such as oxygen vacancy so as it cannot be used as it is. To improve the optical properties dopants need to be added Dopants on ZnO surface can efficiently capture the electrons from the conduction band. These dopants

increases the activity of the catalyst. The dopants may be noble gas, metals such as Pt[20-21], Au[21-23], Ag[24,25] Pd[26]. The Ag is doped with ZnO and this doping is called as p-doping[27-30].

Ag doped ZnO can be prepared by different methods such as sol-gel[31], sonochemical[32]and coprecipitation [33] but those methods requires hard conditions and high cost. So In our study a simple precipitation -decomposition method is used for the synthesis of the Ag-ZnO photocatalyst. This prepared material shows a higher catalytic activity and stability. Ag-ZnO shows a very excellent photocatalytic activity in the photodegratation of dyes (MB) with LED. A possible mechanism is proposed in detail.

2. Experimental

2.1 Materials And Methods

The commercial Metylene Blue (MB), obtained (molecular formula = $C_{16}H_{18}ClN_3S$; molecular mass in amu 319.86 and λ_{max} 644 nm), Oxalic acid dihydrate (99 %) and Zinc nitrate hexahydrate (AR), $AgNO_3$ were obtained from Sigma-Aldrich and Merck were used as received. The entire reagents used analytical grade without further purification Double-distilled water was used to prepare experimental (alkaline $KmnO_4$) solutions. The pH of the solutions are adjusted with acids or bases

2.2 Preparation of Ag–ZnO Catalyst

Precipitation decomposition method is used to prepare Ag-ZnO catalyst . Aqueous solutions of 50 mL of 0.4 M zinc nitrate hexahydrate ($Zn(NO_3)_2.6H_2O$) and 50 mL of 0.6 M oxalic acid dihydrate ($H_2C_2O_4.2H_2O$) in deionized water were brought to the temperature around 70°C separately. 5 mL of 0.1905g of $AgNO_3$ was combined with the zinc nitrate solution. To this mixture ($AgNO_3$ + $Zn(NO_3)_2.6H_2O$) oxalic acid solution was added. Ag–zinc oxalate precipitate is occurred and this solution is made for stirring and heating for 1 hr at 70°C. The solution was brought to room temperature. A fine uniform precipitate of Ag–zinc oxalate was formed. The Ag–zinc oxalate precipitate were washed several times with distilled water, air-dried overnight and dried at 100 °C for 4 hr. The sample was calcined in a muffle furnace to reach the decomposition (450°C) temperature. After 5 hr, the furnace was brought to room temperature. The Ag–ZnO catalyst was collected and used for further analysis. This catalyst contained 3 wt% of Ag. Catalysts with 2 wt% of Ag were prepared by using the above procedure. The bare ZnO was prepared by same method without addition of $AgNO_3$.

2.3 Analytical Methods

Powder X-ray diffraction pattern was obtained using an X'Pert PRO diffractometer equipped with Cu-Ka radiation (wavelength = 1.5406 A ˚) at 2.2 kW (max.). Peak positions were compared with standard files to identify the crystalline phases. The SEM images were taken on a JEOL JSM-6390 model (made in Japan) scanning electron microscope. The EDAX spectrum was recorded by OXFORD INCAPENTAx3 model made in England. Before FE-SEM measurements, the samples were mounted on a gold platform placed in the scanning electron microscope for subsequent analysis at various magnifications, equipped with OXFORD, energy dispersive X-ray microanalysis (EDS). Fourier transform infrared spectrometer. **Make: Thermo Nicolet Model:6700 .** Essential Specification: Wave number range: 4000 to 400 cm -1. **UV-VIS SPECTROPHOTOMETER Make: Varian Model: 2450.** Wave length Range : 190 nm to 900nm;

2.4 Dye Degradation Experiments

Light Emitting Diodes (LED) photocatalytic degradation experiments were carried out under similar Conditions. An open borosilicate glass tube of 1000 mL capacity, 100 cm height, and 5cm diameter was used as the reaction vessel. 500 mL of MB (10^{-5}M) with the appropriate amount Ag-ZnO catalyst were magnetically stirred in the dark for 30mins to attain adsorption-desorption equilibrium between the dye and Ag-ZnO catalyst. After dark adsorption the sample was taken for analysis and then irradiated with LED lights (strip). At specific time intervals, 2–3 mL of the sample was withdrawn and centrifuged to separate the catalyst for the further analysis.

3. Results and Discussions

3.1.1 XRD Analysis

Fig. 1 shows the XRD patterns of synthesized photocatalyst. For the bare ZnO diffraction peaks at 31.68, 34.36, 36.18 and 56.56, correspond to (100), (002), (101) and (110) planes of wurtzite ZnO. No other diffraction peaks are detected in the bare ZnO Nps. For Ag-ZnO Nps, the Ag concentration is very low due to this Ag could not be detected by XRD and the presence of Ag is detected by EDAX. The size of the crystalline is measured and shown in table1.

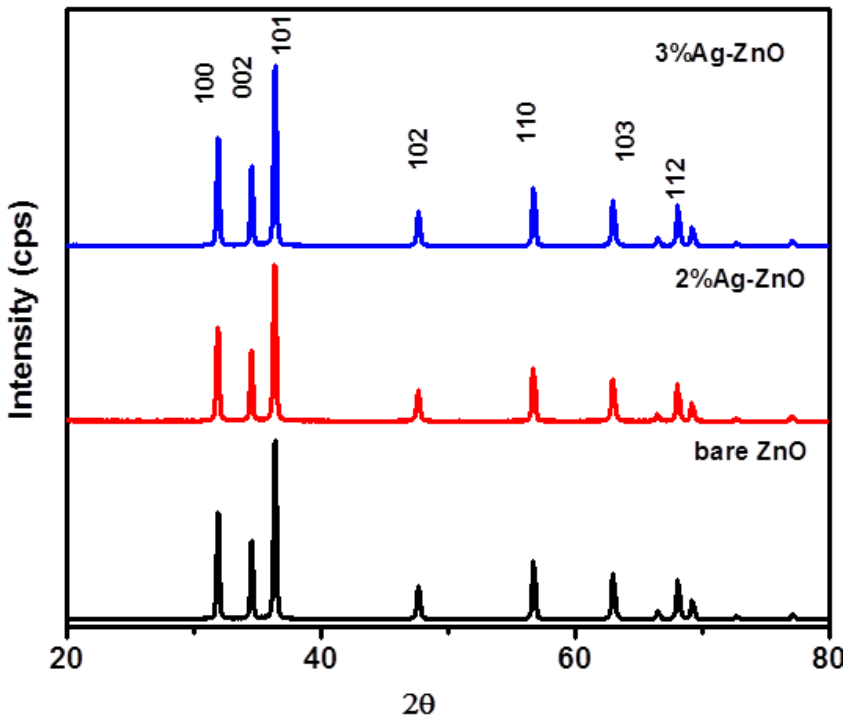

Fig1. XRD patterns of bare ZnO and Ag-ZnO Catalyst

Table I: Geometric parameters of un-doped and Ag-doped ZnO nano catalyst

S.No	Sample Id	(hkl)	Average crystalline size D (nm)
1	ZnO bare	100	45.62
2	1%Ag-ZnO	100	28.32
3	2% Ag-ZnO	100	24.45
4	3% Ag-ZnO	100	22.68

3.1.2 SEM Analysis:

SEM is used to study the surface morphologies of the synthesized catalyst 3%Ag-ZnO by SEM images. The SEM images at different magnifications with different locations of 3%Ag-ZnO are given in (Fig. 2). The rod shaped structure is clearly shown at higher magnification(500nm) for ZnO . At Lower magnification at three different locations (1, 3 & 5 µm) clearly indicates the presence of Ag (indicated by arrow marks). Ag particles are highly dispersed on the surface of ZnO similar observation are observed 3% Ag doped ZnO. EDAX helped to show the elements present in the synthesized catalyst (Ag, Zn and O) (Fig3).

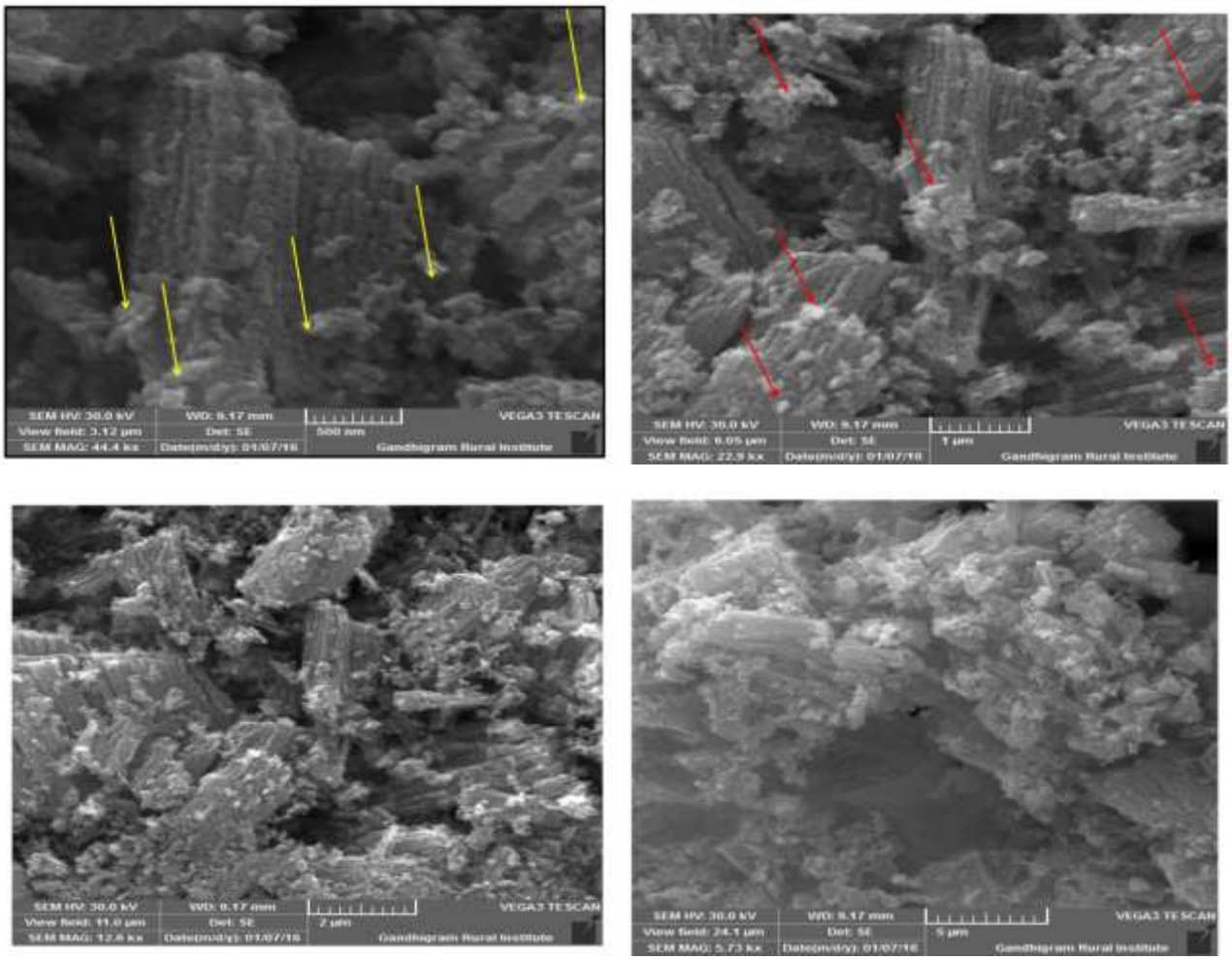

Fig2. SEM images at 3% Ag–ZnO Catalyst at different maganification (500nm, 1µm,3µm,5µm)

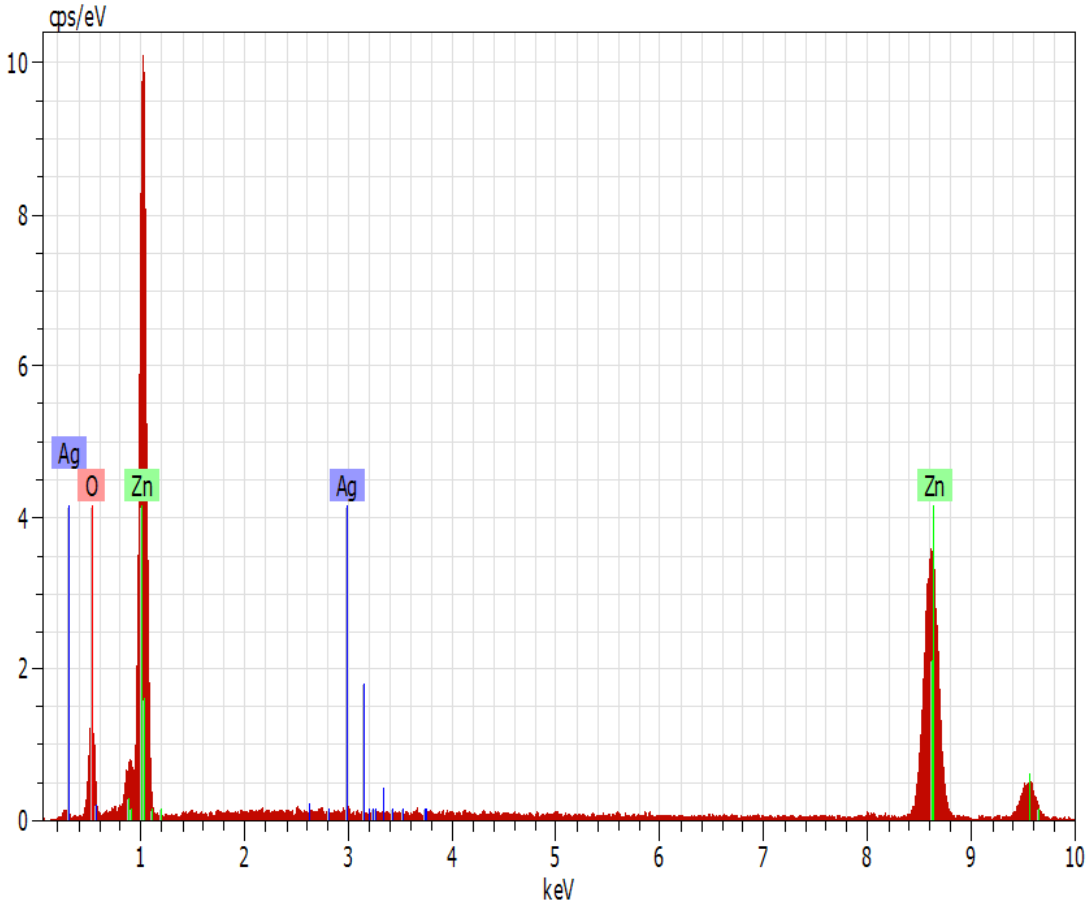

Fig3.EDAX images at 3% Ag-ZnO Catalyst.

3.1.3 UV-Visible SPECTRA

The UV spectra of bare ZnO, Ag doped ZnO catalyst are shown in Fig.4 , respectively. The presence of the dopants shifts the absorbance of the ZnO. The dopants Ag slightly shifts the absorbance of ZnO to the entire visible region. We could note that the light absorption of Ag-ZnO in the visible light range (>400nm) was higher than pure ZnO catalyst.

In semiconductor, the absorption coefficient is a function of the incident photon energy. Near the absorption edge, the absorption coefficient for direct transition is given by [34]:

$\alpha h\theta = A(h\nu - E_g)^n$

where Eg (eV) is the energy gap, hν (eV) is the energy of incident photon and constant A varies for different transitions, and is related to effective mass of carriers, refractive index, oscillator strength and so on. The n is an index which equals 1/2 corresponding to allowed direct transitions [35]. The extrapolation method is usually used to determine the band gap of semiconductors providing that the transition in the semiconductor at certain wavelength scope is direct. In this work, when the index n is 1/2 in above Eq., by using the relationship of reflectivity and transmission with wavelength, we calculated the square of the absorption coefficient as a function of the incident photon energy (as shown in Fig.5). The energy band gap Eg measurement is 3.23 eV. The measured band gap is lower than the bare ZnO. The band gap of Ag-ZnO Nps is 3.12ev whereas for bare ZnO Nanorods is 3.23ev.

3.1.4 Infrared Spectra

FT-IR spectra for different concentrations of silver doping in the range of 300-4000 cm−1 were recorded and the results can be seen in Fig. 6. The appearance of a sharp band at 508 cm^{-1} in the FT-IR spectra confirms the synthesis of ZnO because it is the characteristic absorption band for the Zn– O stretching vibration. A wide peak was in the 3433 cm−1 that was related to the presence of hydroxyl ions (OH) in the ZnO:Ag system. The symmetric and asymmetric bending modes of C=O bonds were in 1630 and 1390cm−1 [36]. There were some bands originated from the presence of water moisture and carbon dioxide in the air in the process of making pellet. The absorption band at 1020 cm−1 could be attributed to bending vibrational modes [37]. According to Fig. 5, a slight shift with doping silver (Ag) is visible. The shift in the position of the band toward lower frequencies can be associated with changes in bond length due to the partial substitution of Ag^{+} ion at the ZnO lattice [38].

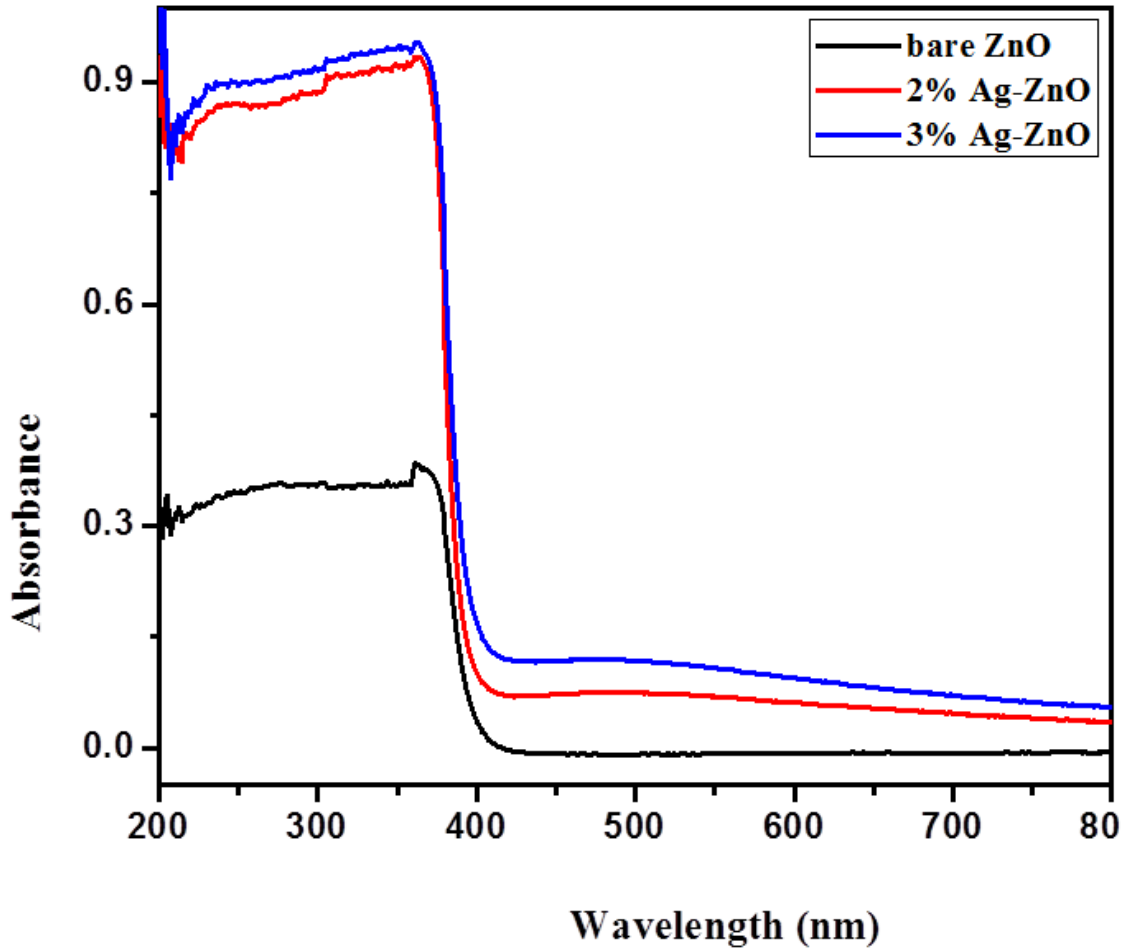

Fig4 UV Spectra of (a) bare ZnO and Ag-ZnO Catalyst.

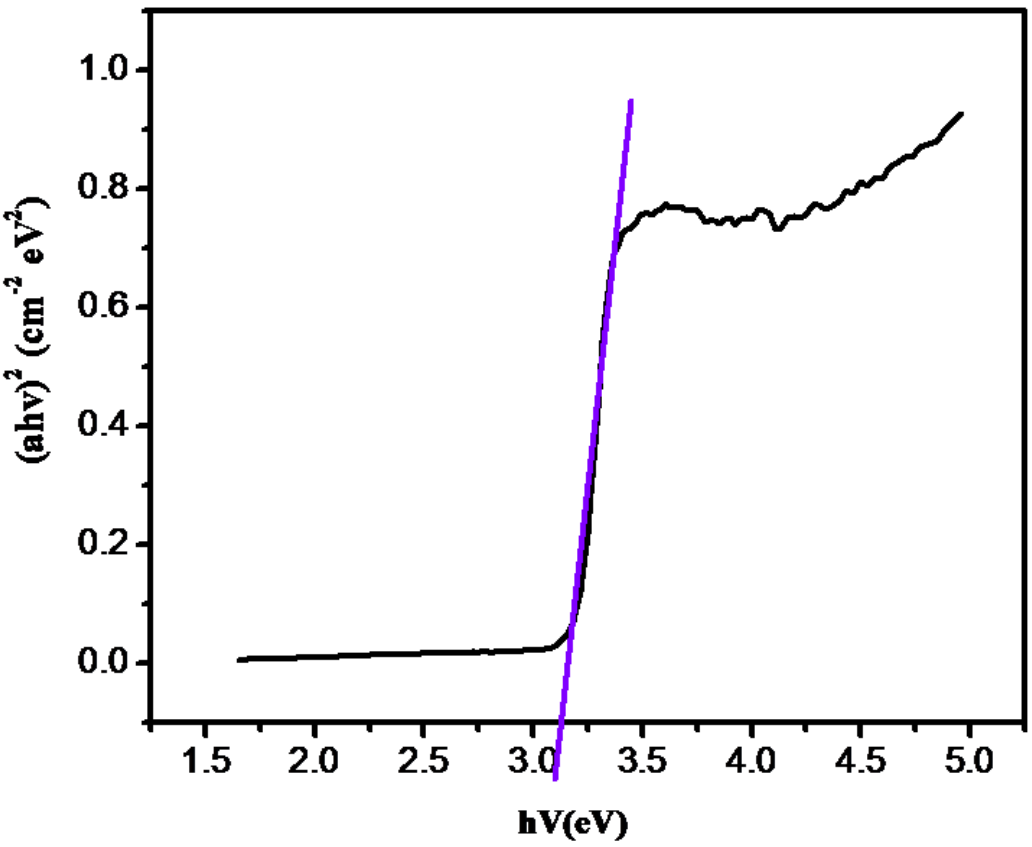

Fig5. Plot for band-gap energy (E_{bg}) of Ag-ZnO

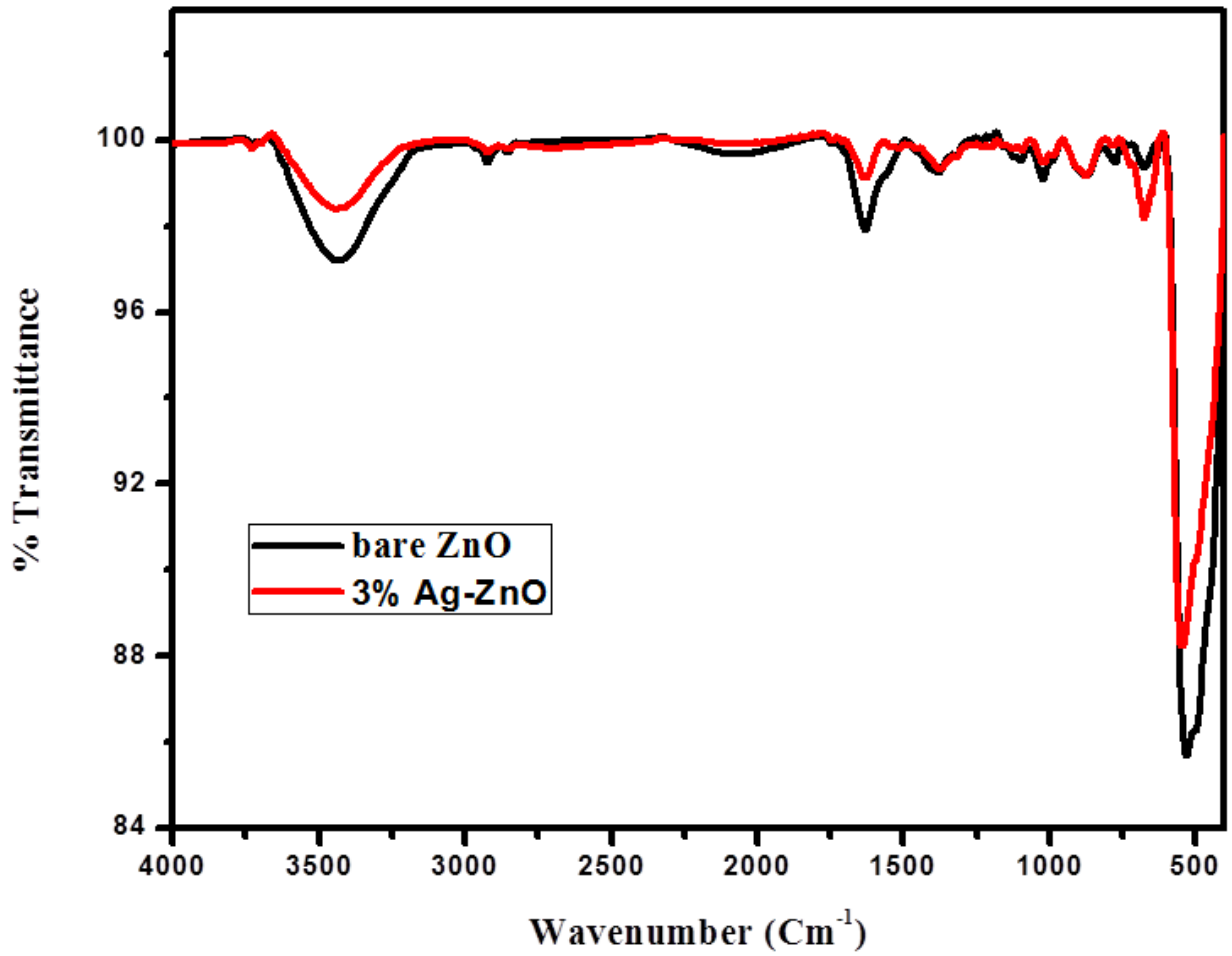

Fig. 6: FTIR spectra for undoped and silver doped ZnO

3.2 Photodegradability of MB

The dye MB is photodegraded with the various photocatalysts under LED irradiation is shown in (Fig. 7). Complete degradation of the dye takes place at the time of 120 min with 3% Ag–ZnO under LED.

In the absence of light with only catalyst 3% Ag-ZnO only 10% decrease in dye concentration could be observed under the similar conditions. This may be due to adsorption of the dye onto the surface of the catalyst. Only 2% degradation was obtained when the reaction was allowed to occur in the presence of LED only. So we can conclude that for the photo degradation both LED light and catalyst are needed. The photocatalysts Ag–ZnO(3% &2%), with various concentrations, TiO_2, bare ZnO, Commercial ZnO, were used under the same conditions. In these 98.2, 71.3, 64.2, 58.3, 56.2% degradations occurred, respectively. This shows that 3%Ag-ZnO catalyst is more efficient than compared to related catalysts in MB degradation.

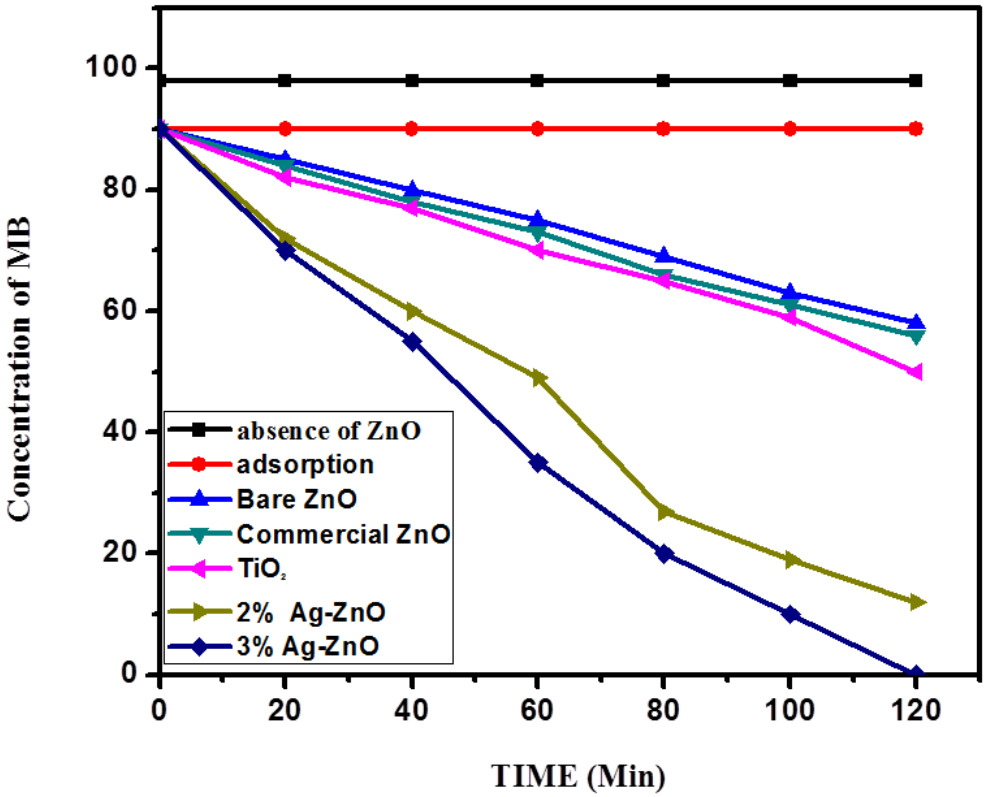

Fig7.Photodegradability of MB; dye concentration = 10^{-5}mol L^{-1}Catalyst suspension = 0.5 g L^{-1}, pH = 11 with ZnO bare and Ag doped ZnO Catalyst.

3.2 Influence of Operational Parameters

pH can play a vital role in photodegradation . The percentage of degradation increased (11.8 to 96.01 %) when the pH increased linearly from 3 to 11 (fig 8). The percentages of degradation of MB at pH 3, 5, 7, 9 and 11 were found to be 11.8, 18.72, 35.71, 45.67, 96.01%, respectively after attainment of adsorption equilibrium (30 min) in all reactions. The adsorption and degradation is high at pH 11.

Experiments performed with different amounts of 3%Ag–ZnO Nps showed that the photodegradation efficiency decreased with an increase in the amount 0.5 to 2.5 gL^{-1} (Fig 9). The suitable catalyst loading for this photodegradation was found to be 0.5gL^{-1}. The decrease in the degradation efficiency of MB for higher amounts may be due to tyndal effect by the catalyst. Similar results are obtained for photodegradation of dyes by bare ZnO [39].

The effect of various initial dye concentrations on the degradation of MB with 3%Ag–ZnO Nps was investigated. Increase of dye concentration from 0.5 to 2.5X10^{-5}molL^{-1} decreased the percentage of degradation from 97.6 to 63 % for 120 min of irradiation (Fig. 10). As the initial concentration of the dye increases, the path length of the photons entering the solution decreases, this also leads to the decrease in photo catalytic degradation efficiency [40].

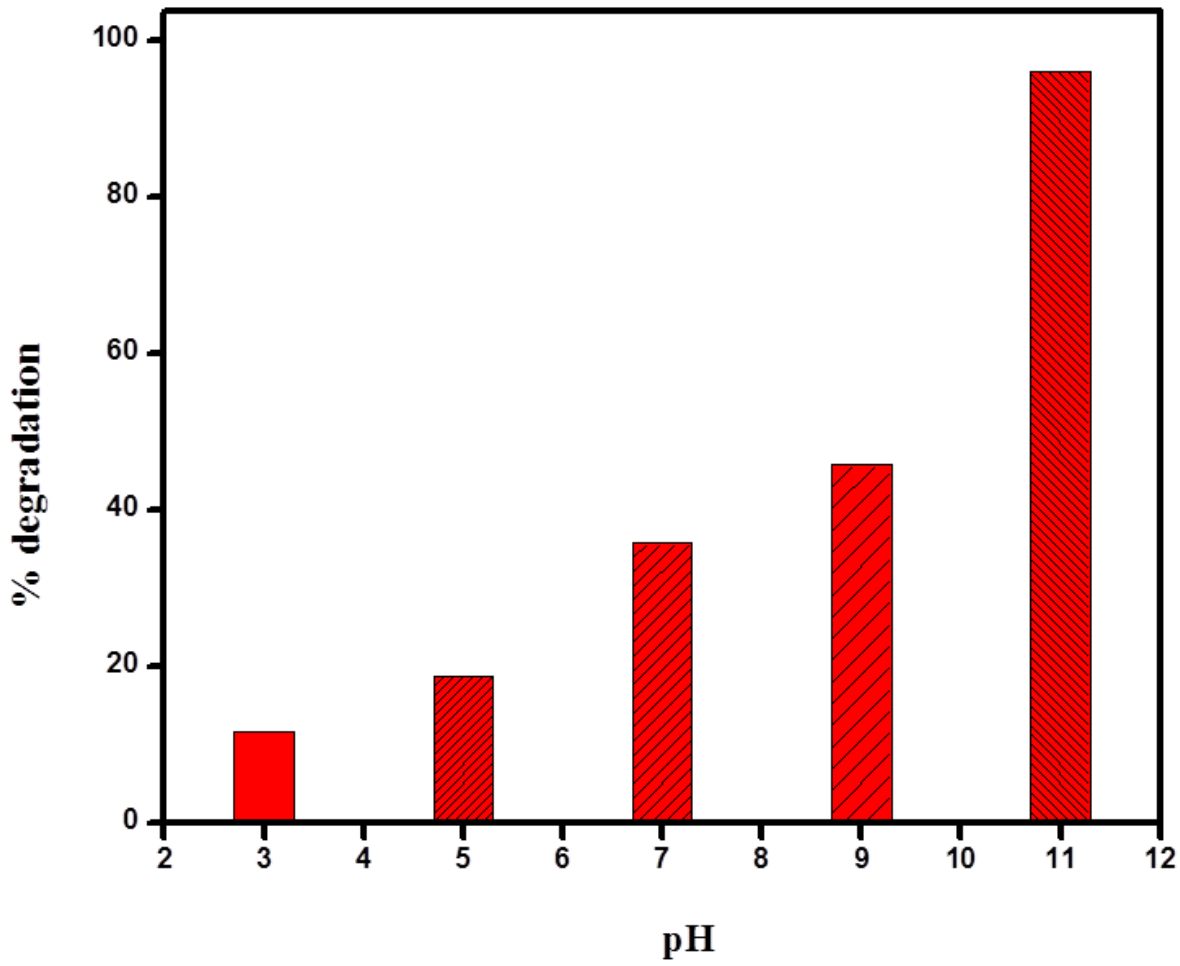

Fig8.Effect of solute ion pH; [MB] = $10^{-5}ML^{-1}$, 3 wt% Ag–ZnO Suspended = 500m g L^{-1}, irradiation time = 120 min.

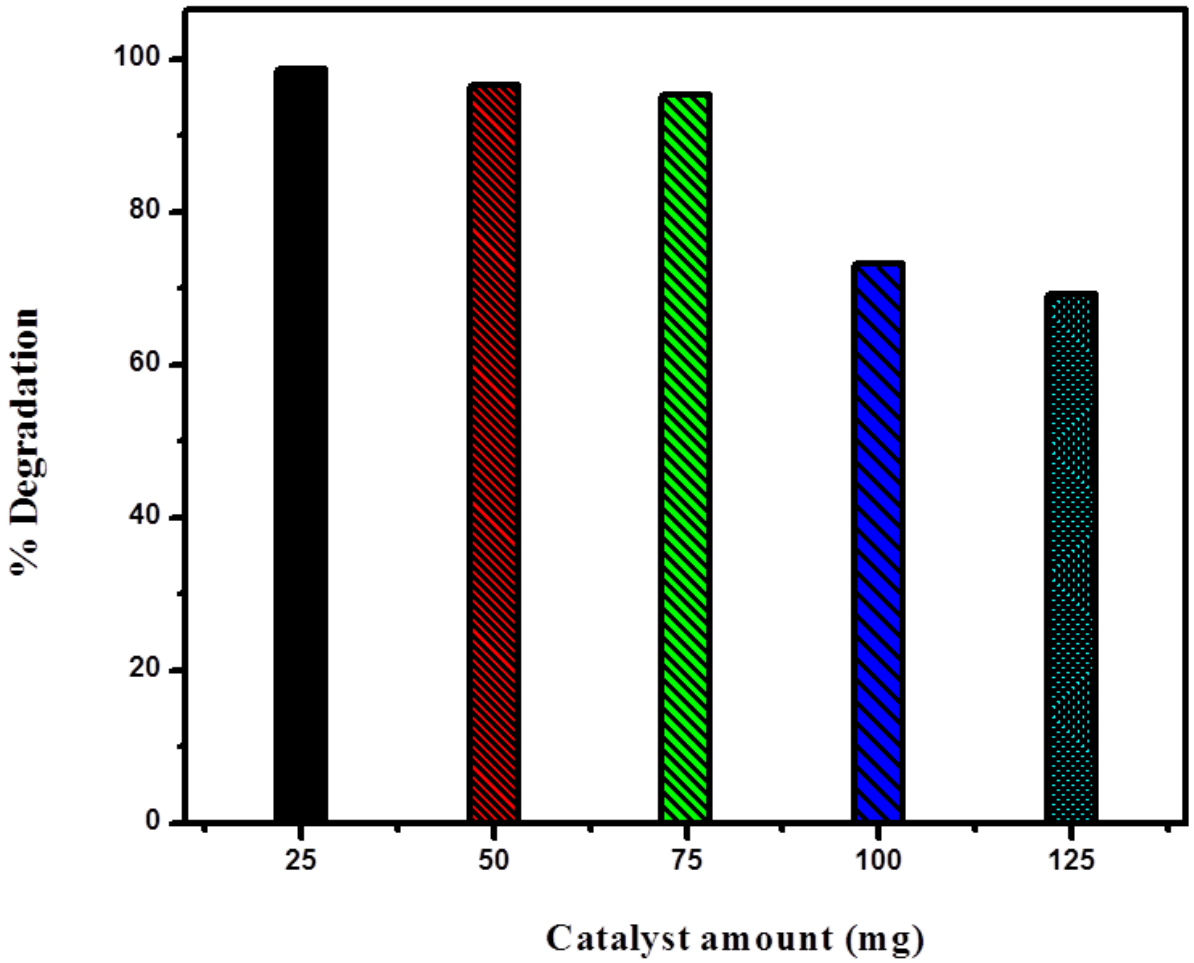

Fig9.Effect of catalyst loading, [MB]=10^{-5}mol L^{-1}, catalyst used =3 wt% Ag–ZnO, pH = 11 irradiation time = 120 min.

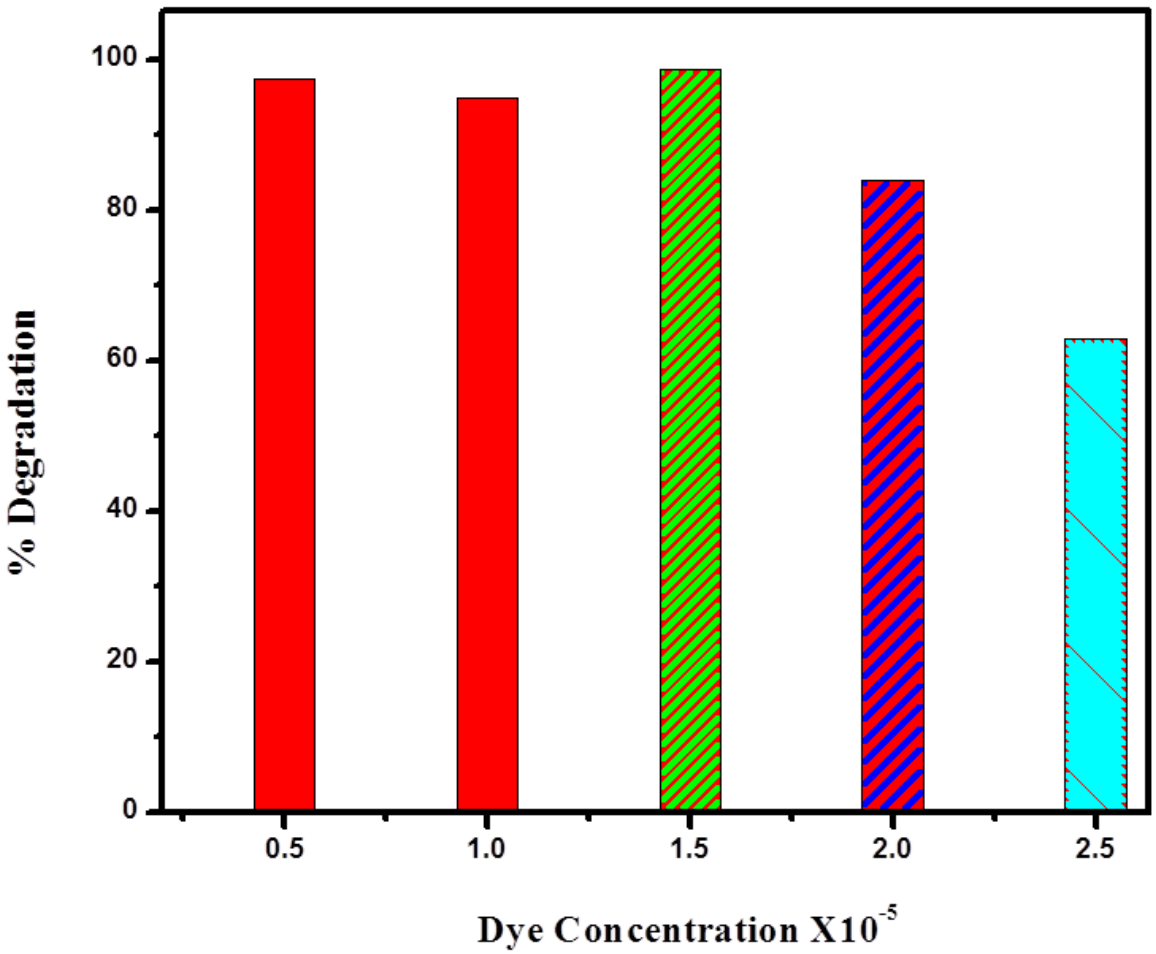

Fig10. The effect of initial concentration of MB on irradiation with LED light in the presence 3% Ag–ZnO; pH = 11catalyst suspension = 0.50 gL^{-1} at different initial concentration.

3.5 Mechanism of Photo Degradation

The results of photocatalytic measurements of the Ag-ZnO catalyst are shown in scheme1. Pure ZnO nanocatalyst showed a significant photocatalytic activity. Under the irradiation of the LED light the electrons are excited to the conduction band from the valence band leaving a hole in the valence band. The electron holes are recombined to reduce the photocatalytic property of semiconductors. This is the reason why we are using dopants (Ag) with ZnO Nps. These dopants help in increasing the photocatalytic properties. The Ag traps the electron in conduction band and reduces the recombination of electron-hole pair. So the electron hole recombination suppressed and Photocatalytic acivity is increased by doping Ag which leads to the oxygen vacancy defect concentration. In sliver doped catalyst the Zn vacancies were more than the oxygen vacancies since sliver is doped in the lattice point of Zinc. So, Zn vacancies accompanied by oxygen vacancies could be responsible for the degradation process. In the absence of LED, by dispersing Ag-ZnO nanocatalyst in the MB solution adsorption and desorption takes place for 30 minutes, during this adsorption and desorption of the catalyst the surface electrons of the Ag nanocatalyst were transferred to the MB. Under LED radiation the electrons from the valence band of ZnO is excited to conduction band producing equal number of holes in valence band. Because the conduction band energy level of ZnO nanocatalyst is higher than that of the Fermi level of Ag-ZnO nanocatalyst, Electrons can flow from ZnO nanocatalyst to Ag nanoparticle. So, oxygen vacancy defects and Ag on the surface of ZnO nanocatalyst trap electrons and prevent the recombination of $e^{-}h^{+}$ pairs. The MB molecules transfer electrons to the conduction band (CB) of ZnO and the Fermi level of Ag when it is radiated with LED lights. Then CB electrons react with dissolved oxygen in the solution to produce superoxide radicals($\cdot O_2^-$). During this time the photogenerated h_{vb}^+ can transfer the charge to the adsorbed water molecule or with surface bound hydroxide species by capturing the catalyst surface to generate active $^{\bullet}OH$.

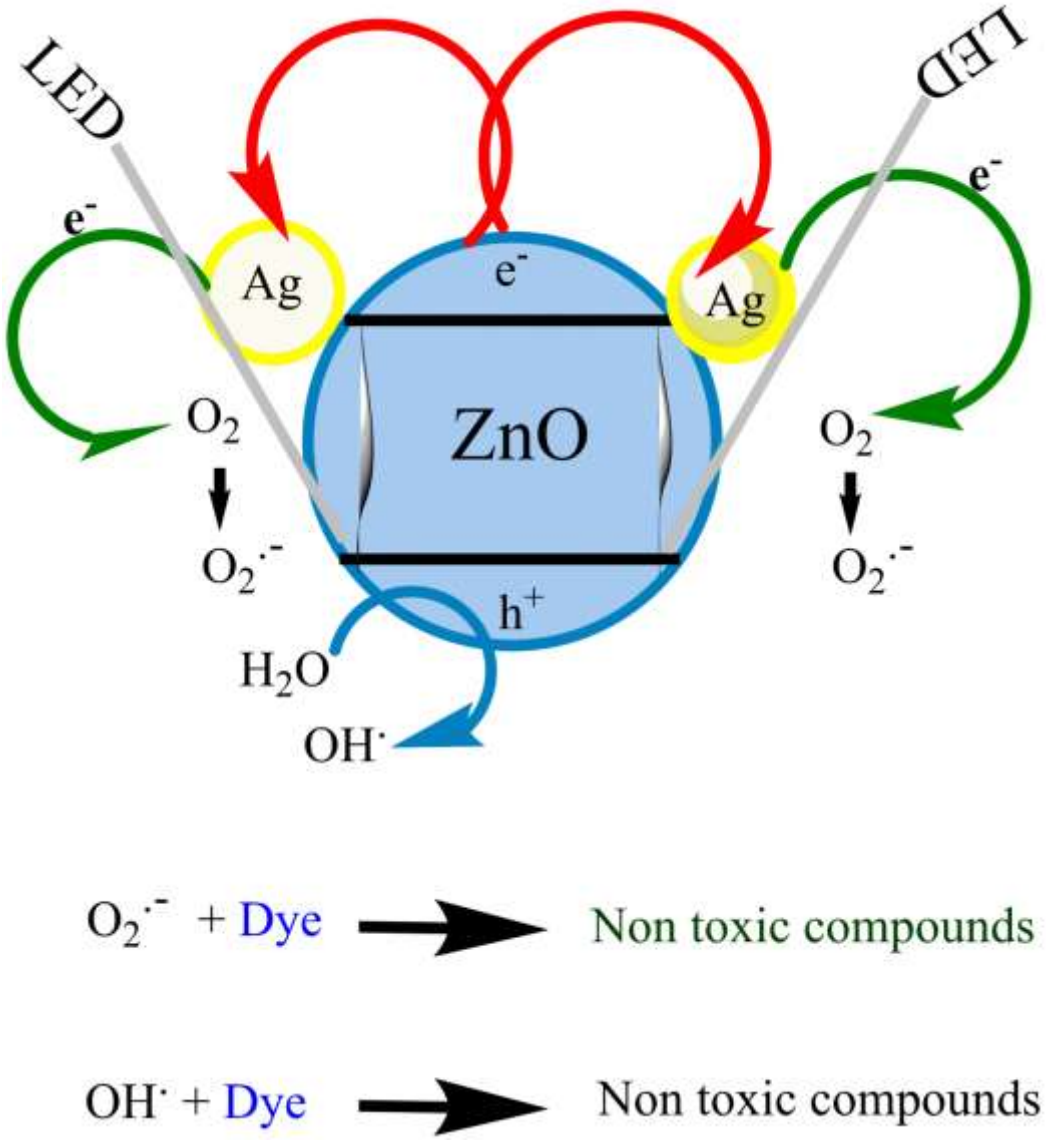

Scheme 1. Enhanced photocatalytic Activity Mechanism of Ag-ZnO in present of light emitting diodes.

4. Conclusion

The Ag-ZnO catalysis is successfully prepared by precipitation decomposition method. The characterisation is studied by XRD, SEM, EDS, UV, IR. The dopant shifts the absorption of Zno catalyst. This lowered reflectance increases absorption in visible region. IR shows the stretching frequency of the catalyst and also study the purity. The role of the dopant Ag trap the photo excited electron by reducing the electron hole recombination which increases the photocatalytic properties. 3%Ag-ZnO nano catalyst shows excellent photocatalytic activity than 2%Ag-ZnO, 1%Ag-ZnO, Ag-ZnO, bare ZnO Nps for the degradation of Methylene Blue dye under LED light. A clear mechanism is proposed where the Ag traps the electron to explain the photocatalytic activity of the catalyst.

Acknowledgements

The author SJS is thankful to the management and principal of St. Josephs college Tiruchirappalli-620002 for their support and encouragement. The authors YJJ and MM are thankful to the management and principal of BWDA Arts and Science College Tindivanam-604304 for providing lab facilities.

References

1. Matthews R.W., Photooxidative degradation of coloured organics in water using supported catalysts. TiO_2 on sand, Water Res., 1991, 25, 1169-1176.
2. Pan H.M. Feng J.H. He G.X. Cerniglia C.E. Chen H.Z., Evaluation of impact of exposure of Sudan azo dyes and their metabolites on human intestinal bacteria, Anaerobe., 2012, 18, 45-453.
3. Sharma A. Rao P. Mathur R.P. Ameta S.C.A., Photocatalytic reactions of xylidine ponceau on semiconducting zinc oxide Powder, J. Photochem. Photobiol.A: Chem., 1995, 86, 197-200.
4. Sakthivel S. Neppolian B. Shankar M.V. Arabindoo B. Palanichamy M., Solar photocatalytic degradation of azo dye: comparison of photocatalytic efficiency of ZnO and TiO_2, Sol. Energy Mater. Sol. Cells., 2003, 30, 65–82
5. Murugesan V., Solar photocatalytic degradation of azo dye: comparison of photocatalytic efficiency of ZnO
6. and TiO_2, Sol. Energy Mater. Sol. Cells., 2003, 77, 65-82.
7. Linsebigler A.L. Lu G.Q. Yates J.T., Photocatalysis on TiO_2 surfaces: principles, mechanisms, and selected results Chem. Rev., 1995, 95, 735-758.
8. Thompson T.L. Yates J.T., Surface science studies of the photoactivation of TiO_2 new photochemical Process, Chem. Rev., 2006, 106, 4428-4453.
9. Kim S. Choi W., Visible-Light-Induced Photocatalytic Degradation of 4-Chlorophenol and Phenolic Compounds in Aqueous Suspension of Pure Titania: Demonstrating the Existence of a Surface-Complex-Mediated path, J. Phys. Chem. B., 2005, 109, 5143-5149.
10. Zhang G.K. Ding X.M. He F.S. Yu X.Y. Zhou J. Hu Y.J. Xie J.W., Low-temperature synthesis and photocatalytic activity of TiO_2 pillared montmorillonite, Langmuir., 2008, 24, 1026-1030.
11. Surolia P. K. Lazar M. A. Tayade R. J. Jasra R. V., Photocatalytic Degradation of 3,3′-Dimethylbiphenyl-4,4′-diamine (o- Tolidine) over Nanocrystalline TiO_2 Synthesized by Sol−Gel, Solution Combustion, and Hydrothermal Methods, Ind Eng Chem Res., 47, 5847-5865.
12. Lazar M. A. Tayade R. J. Bajaj H. C. Jasra R. V., Correlation of Surface Properties and Photocatalytic Activity of Nano crystalline TiO_2 on the Synthesis Route. Nano Hybids., 2012, 1, 57-80.
13. Chen H. W. Ku. Y. Wu C. Y., Effect of LED optical characteristics on temporal behavior of o-cresol decomposition by UV/TiO_2 process. J Chem Technol Biotechnol., 2007, 82, 626-635.
14. Daniel D. Gutz I. G. R., Microfluidic cell with a TiO_2-modified gold electrode irradiated by an UV-LED for in situ photocatalytic decomposition of organic matter and its potentiality for voltammetric analysis of metal ions. Electrochem Commun., 2007, 9,522-528.
15. Wan-Kuen Jo. Rajesh J. Tayade., Recent developments in photocatalytic dye degradation upon irradiation with energy-efficient light emitting diodes. Chinese Journal of Catalysis., 2014, 35,1781-1792.
16. Hu J. S. Ren L. L, Guo Y. G, Liang H. P, Cao A. M, Wan L. J, and Bai C. L., Mass production and high photocatalytic activity of ZnS nanoporous nanoparticles. Angew Chem Int Ed., 2005, 44, 1269-1273.
17. Fujishima A. and Honda K. Electrochemical Photolysis of Water at a Semiconductor Electrode. Nature., 1972, 238,37-38.
18. Linsebigler A. L, Lu G. Q, and Yates T. J., Photocatalysis on TiO2 Surfaces: Principles, Mechanisms, and Selected Results, Chem Rev., 1995, 95, 35-738
19. Pemmaraju C.D, Hanafin R. Archer T. Braun H.B, Sanvito S., Impurity-ion pair induced high-temperature ferromagnetism in co-doped zno, Phys. Rev. B., 2008, 78, 054428.
20. Sarsari I.A, Pemmaraju C.D, Salamati H. Sanvito S., Many-body quasiparticle spectrum of co-doped zno: perspective, Phys. Rev. B 87 (2013) 245118.
21. Sclafani A. Palmisano L. MarcI´ 0 G, and Venezia A. M., Influence of platinum on catalytic activity of polycrystalline WO_3 employed for phenol photodegradation in aqueous suspension, Sol. Energy Mater. Sol. Cells., 1998, 51, 203-219.
22. Sakthivel S. Shankar M V. Palanichamy M. Arabindoo B. Bahnemann D. W, and Murugesan V., Enhancement of photocatalytic activity by metal deposition: characterisation and photonic efficiency of Pt, Au and Pd deposited on TiO_2 catalyst. Water Res., 2004, 38, 3001-3008

23. Wang C. Liu C. Zheng X. Chen J. and Shen T., The surface chemistry of hybrid nanometer-sized particles I. Photochemical deposition of gold on ultrafine TiO_2 particles. Colloids Surf. A., 1998, 131, 271-280
24. Li X. Z, and Li F. B, Study of Au/Au^{3+}-TiO_2 photo catalysts toward visible photo oxidati****on for water and wastewater treatment. Environ Sci Techno., 2001, 35, 2381-2388.
25. Sclafani A. and Hermann J. M, Influence of metallic silver and of platinum-silver bimetallic deposits on the photocatalytic activity of titania (anatase and rutile) in organic and aqueous media. J Photochem Photobiol. A., 1998, 113, 181-188.
26. Tran H. Chiang K. Scott J. and Amal R., Understanding selective enhancement by silver during photocatalytic oxidation. Photochem. Photobiol. Sci 4, 565-567.
27. Wang C. M, Heller A. and Gerischer H, Palladium catalysis of O_2 reduction by electrons accumulated on TiO_2 particles during photoassisted oxidation of organic compounds. J Am Chem Soc., 1992, 114, 5230-5234
28. Sahu D. Panda N. Acharya B. Panda A., Enhanced uv absorbance and photoluminescence properties of ultrasound assisted synthesized gold doped zno nanorods, Optical Materials 2014, 36, 1402–1407.
29. Yan Y. Al-Jassim M. Wei S.H., Doping of zno by group-ib elements, Applied physics letters., 2016, 89, 181912–181912.
30. Ma Y, Du G T, Yang S.R. Li Z.T, B. J. Zhao, X. T. Yang, T. P. Yang, Y. T. Zhang, Liu D.L., Control of conductivity type in undoped zno thin films grown by metalorganic vapor phase epitaxy, Journal of Applied Physics., 95, 11.
31. Thomas M. Sun W. Cui J., Mechanism of ag doping in zno nanowires by electrodeposition: experimental and theoretical insights, The Journal of Physical Chemistry C 116 ., 2012, 10, 6383–6391.
32. Rad M.S, Kompany A. Zak A.K, Javidi M. Mortazavi S., Microleakage and antibacterial properties of zno and zno: Ag nanopowders prepared via a sol–gel method for endodontic sealer application, Journal of nanoparticle research., 2013, 15 , 9, 1–8.
33. Karunakaran C. Rajeswari V. Gomathisankar P., Antibacterial and photocatalytic activities of sonochemically prepared zno and Ag-Zno, Journal of Alloys and Compounds 2010, 508, (2) , 587–591.
34. Chauhan R. Kumar A. Chaudhary R.P. Synthesis and characterization of silver doped zno nanoparticles., Archives of Applied Science Research., 2010, 2, (5) 378–385.
35. Sze S.M, Ng K.K., Physics of semiconductor devices, Wiley. com, 2006.
36. Li F. Liu C. Ma Z. Zhao L., New methods for determining the band gap behavior of ZnO, Optical Materials., 2012, 34 1062-1066.
37. Zandi S. Kameli P. Salamati H. Ahmadvand H. Hakimi M., Microstructure and optical properties of zno nanoparticles prepared by a simple method, Physica B: Condensed Matter., 2011, 406, (17) 3215–3218.
38. Lanje A.S, Sharma S.J, Ningthoujam R.S, Ahn J.S, Pode R.B., Low temperature dielectric studies of zinc oxide (zno) nanoparticles prepared by precipitation method, Advanced Powder Technology., 2013, 24 (1) 331–335.
39. Murtaza G. Ahmad R. Rashid M. Hassan M. Hussnain A. Khan M.A, Ehsan ul Haq M. Shafique M. Riaz S., Structural and magnetic studies on zr doped zno diluted magnetic semiconductor, Current Applied Physics., 2014, 14 (2) 176–181.
40. Krishnakumar B. Selvam K. Velmurugan R Swaminathan M., Influence of operational parameters on photodegradation of Acid Black 1 with ZnO. Desalin Water Treat., 2012, 24,132-139.
41. Krishnakumar B. Subash B. Swaminathan M., Photocatalytic destruction of phenol by TiO_2 powders. Purif. Technol., 2012, 85, 35-44.

*****